

Structure functions and energy dissipation dependence on Reynolds number

G. Boffetta¹ and G.P. Romano²

¹ *Dipartimento di Fisica Generale and INFN, Università di Torino,*

Via Pietro Giuria 1, I-10125 Torino, Italy

² *Dipartimento di Meccanica ed Aeronautica, Università di Roma "la Sapienza",*

Via Eudossiana 18, I-00184 Roma, Italy

(October 31, 2018)

Abstract

The dependence of the statistics of energy dissipation on the Reynolds number is investigated in an experimental jet flow. In a range of about one decade of Re_λ (from about 200 to 2000) the adimensional mean energy dissipation is found to be independent on Re_λ , while the higher moments of dissipation show a power-law dependence. The scaling exponents are found to be consistent with a simple prediction based on the multifractal model for inertial range structure functions. This is an experimental confirmation of the connection between inertial range quantities and dissipation statistics predicted by the multifractal approach.

I. INTRODUCTION

There is considerable experimental [1] and numerical [2] evidence that the longitudinal velocity difference structure functions

$$S_q(\ell) \equiv \langle \delta u(\ell)^q \rangle = C_q \langle \varepsilon \rangle^{q/3} \ell^{q/3} \left(\frac{\ell}{L} \right)^{\zeta_q - q/3} \quad (1)$$

are affected by intermittency corrections in the scaling exponents ζ_q which deviate from the Kolmogorov self-similar prediction $\zeta_q = q/3$ [3,4] (C_q is a constant possibly depending on the Reynolds number, ε is the turbulent kinetic energy dissipation, ℓ is a generic length scale and L is the integral length scale). The estimate of ζ_q is now available for a wide range of Reynolds numbers and different flow configurations. The analysis of experimental data show that structure functions display the scaling behavior (1) for sufficiently high Reynolds number, Re , and that in such conditions the longitudinal exponents ζ_p become independent on Re [5,6]. There is also experimental support for the scaling exponents to be Re -independent also at small Re (when the scaling behavior in (1) is even not observable) if one make use of the so-called extended self similarity analysis (ESS) [7]. However, the precise relation between this empirical result and the classical scaling behavior (1), expected from dimensional arguments, is not well understood. We will not further discuss this point here.

The basic fundamental property of fully developed turbulence is that the average energy dissipation $\langle \varepsilon \rangle$ entering in (1) is asymptotically Re -independent, when adimensionalized with large scale variables [3,8,9]. On the other hand, it is well known that the statistics of the local energy dissipation, which assuming isotropy can be defined in terms of its 1D surrogate

$$\varepsilon(x) = 15\nu \left(\frac{\partial u}{\partial x} \right)^2, \quad (2)$$

strongly depends on Re , becoming more and more intermittent with increasing Re [10,11]. This effect is also reflected in the tails of the pdf of velocity increments at very small

separations [12–14]. A statistical description of the behavior of the local energy dissipation (2) can be obtained in terms of quantities defined in the inertial range, such as (1), within the multifractal approach. This approach, originally introduced as a phenomenological model for the inertial range statistics [15,16], has been extended to the prediction of dissipative scale statistics [4,17]. In particular, this approach predicts a scaling behavior of the moments of (2) with Re [18], which has been recently measured in a simplified model of turbulence [21].

In the present paper we investigate the Reynolds dependence of the statistics of (2) in an experimental water jet. We have examined a series of data obtained from LDA measurements which cover about one decade of Reynolds numbers. The quality of the statistics allows us to compute high order structure functions with reasonable accuracy and to partially resolve the dissipative scales. Our main result is that the dependence of the statistics of dissipation on the Reynolds number is found to be consistent with the multifractal prediction obtained by assuming a fluctuating dissipative scale.

The remaining of the paper is organized as follows. In Section II we introduce the theoretical models for the statistics of dissipation. In Section III, the experimental set-up and the data analysis procedure. Section IV is devoted to the presentation of the results, whereas concluding remarks are given in Section V.

II. MULTIFRACTAL DESCRIPTION OF ENERGY DISSIPATION

A phenomenological description of intermittency is given by the multifractal model [15]. This model introduces a continuous set of scaling exponents h which locally relates the velocity fluctuations at scale ℓ entering in (1) with a large scale velocity fluctuation u' :

$$\delta u(\ell) \sim u' \left(\frac{\ell}{L} \right)^h. \quad (3)$$

The local exponent h is realized with a probability which scales with $(\ell/L)^{Z(h)}$ where $Z(h)$ is the codimension of the fractal set on which the h -scaling holds. The scaling exponent of structure functions (1) are obtained by a steepest descent argument over h :

$$\zeta_q = \inf_h [qh + Z(h)] . \quad (4)$$

The scaling region of (3) is bounded from below by the Kolmogorov dissipative scale η at which dissipation starts to dominate, i.e. at which the local Reynolds number is of order 1:

$$\frac{\eta \delta u(\eta)}{\nu} \simeq 1 . \quad (5)$$

From (3) and (5) one obtains that in the multifractal description of intermittency the dissipative scale is a fluctuating quantity, i.e. depends on the local scaling exponent h according to

$$\eta \sim L \left(\frac{u' L}{\nu} \right)^{-\frac{1}{1+h}} \sim L Re_\lambda^{-\frac{2}{1+h}} \quad (6)$$

where $Re_\lambda = u' \lambda / \nu$ is the Reynolds number based on the Taylor microscale $\lambda = \sqrt{15 \nu u'^2 / \langle \varepsilon \rangle}$.

Below the dissipative scale the flow can be assumed smooth and one can replace the derivative in (2) with

$$\varepsilon = 15 \nu \left(\frac{\delta u(\eta)}{\eta} \right)^2 . \quad (7)$$

Assuming that the multifractal model can be pushed down to the dissipative scale, one can evaluate the statistics of (2) by inserting (3) and (6) into (7). One ends with the expression [18,4,21]

$$\langle \varepsilon^p \rangle \sim \langle \varepsilon \rangle^p \int d\mu(h) Re_\lambda^{-2[3ph-p+Z(h)]/(1+h)} \sim \langle \varepsilon \rangle^p Re_\lambda^{-2\theta_p} \quad (8)$$

where again the integral has been evaluated by a steepest descent argument as

$$\theta_p = \inf_h \left[\frac{3ph - p + Z(h)}{1 + h} \right] \quad (9)$$

The standard inequality in the multifractal model (following from the exact result $\zeta_3 = 1$), $Z(h) \geq 1 - 3h$ [4], implies for (9) $\theta_1 = 0$ which is nothing but the request of finite non-vanishing dissipation in the limit $Re \rightarrow \infty$. For $p > 1$, $\theta_p < 0$, i.e. the tail of the distribution of ε becomes wider with the Reynolds number.

Let us remark that the prediction (9) is based on the assumption of a fluctuating dissipative scale η according to (6). If one assume, on the contrary, that dissipation enters in (7) as an average quantity one ends up with a different predictions for the exponents θ_p [3,19]. Numerical simulations with a simplified model of turbulent cascade have shown that the exponents (6) are indeed observed and the alternative prediction is ruled out [21]. In the next Section, we will see that also our experimental data are in agreement with prediction (9).

In the following we will consider data analysis of one component of the velocity in water jets at different Reynolds numbers. Because of the discretization of the acquisition, we are forced to replace spatial derivatives with velocity differences at small scales. The key quantity for our discussion is a generalization of (2) over a finite scale ℓ :

$$E(\ell) \equiv 15\nu \left(\frac{\delta u(\ell)}{\ell} \right)^2. \quad (10)$$

$E(\ell)$ is a convenient definition of surrogate energy dissipation if the scale ℓ is sufficiently small. The average dissipative scale dependence on Reynolds number can be obtained from (7) and (1) as

$$\bar{\eta} \simeq LRe_\lambda^{-\frac{2}{2-\zeta_2}}. \quad (11)$$

In the analysis of experimental data it is convenient to normalize separations with $\bar{\eta}$ and we will consider (10) at fixed $\ell^* = \ell/\bar{\eta}$.

In the limit of very small separations (i.e. $\ell^* \simeq 1$) (10) recovers the finite difference representation of the 1D-energy dissipation (7) and thus, from (8)

$$\frac{\langle E(\ell)^p \rangle}{\langle E(\ell) \rangle^p} = \frac{\langle \varepsilon^p \rangle}{\langle \varepsilon \rangle^p} \simeq Re_\lambda^{-2\theta_p} \quad (12)$$

with the exponents θ_p given by (9).

In the case of separations in the inertial range, from (1) we have $\langle E(\ell)^p \rangle / \langle E(\ell) \rangle^p \simeq \ell^{\zeta_{2p} - p\zeta_2}$. Because $\ell = \ell^* \bar{\eta}$, using (11) we end with the prediction

$$\frac{\langle E(\ell)^p \rangle}{\langle E(\ell) \rangle^p} \simeq Re_\lambda^{-\frac{2\zeta_{2p} - 2p\zeta_2}{2-\zeta_2}} \quad (13)$$

Let us remark that the exponents in (12) and (13) are expected to be not very different (they are both zero for non-intermittent turbulence) and thus a discrimination between the two prediction require good accuracy.

III. EXPERIMENTAL SET-UP AND DATA ANALYSIS

The experimental setup consists of a water jet in a closed circuit facility as shown in Figure 1. A centrifugal pump moves water from a primary tank into a settling chamber which is equipped with a valve to damp oscillations due to the pump. A series of contractions leads to a 1.5 m long pipe, with an inner diameter of 14 cm which is followed by the final contraction (1:50 in area) to the jet. The jet (diameter $d = 20$ mm) exits into a large water-filled tank (height $30d$, width $30d$, length $60d$) from which the water returns to the primary tank. The pipe, the contraction and large tank are made of perspex to allow optical access to the flow. At the jet exit, the flow is axisymmetric and has no swirl; preliminary measurements also confirmed that it is unaffected by any external forcing due to the pump. The jet has a top-hat velocity profile at the nozzle exit with a boundary layer shape parameter (defined as the ratio between the displacement and momentum thickness at the outlet) equal to 3.29 and a turbulent intensity equal to about 0.021 on the jet axis.

Velocity measurements are performed by means of a forward-scatter Laser Doppler Anemometer (LDA) equipped with two Bragg cells. The fringe spacing is $3.416 \mu\text{m}$ and the measurement volume size is about 0.1 mm , 0.1 mm , 0.8 mm along the x , y and z axes respectively. The LDA data are randomly distributed in time; therefore, they are resampled by using a linear interpolation to obtain evenly spaced samples and also to provide unbiased statistics [22]. The value of Re_λ is sufficiently large to expect the LDA noise not to affect the behavior of structure functions in the IR [23]. The LDA data on longitudinal and transverse structure functions and on scaling exponents were compared to data obtained by Hot Wire Anemometry in a similar jet; the agreement was good up to 8^{th} order [22].

Measurements were made at $x/d \simeq 40$ (x is measured from the nozzle exit plane), where

the flow field may be considered to be approximately self-preserving and isotropic [23]. The jet exit velocity U_0 was selected so that the exit Reynolds number $Re_d \equiv U_0 d / \nu$ changes from about 2×10^4 to 2×10^5 . As a consequence, Re_λ changes from about 200 to almost 2000 at the measurement location. The number of collected samples is about 10^6 in each run. As usually done in practice, we resort to Taylor hypothesis to transform time differences into space differences by means of the local mean velocity U . The number of independent samples, given by $UT_S/2L$ (where T_S is the total record duration), is about 10^4 . Probability density functions of the longitudinal velocity increments have been calculated at different values of ℓ^* . The distributions indicate that the number of samples is adequate for achieving a closure of the integrand associated with the structure functions $S_q(\ell)$ at least up to $q = 8$. In Table I we summarize some parameters of the experiments.

Because the acquisition rate is constant for the different runs ($\delta t = 5 \times 10^{-4}$ s) the smallest resolved scale $\delta x = U\delta t$ varies with Re_λ . By increasing Re_λ we have both an increasing of δx (as Re_λ^2) and a decreasing of the dissipative scale $\bar{\eta}$ according to (11). Despite these limitations, we are confident that are able to resolve, at least partially, the dissipative range in all the reported runs. In the extreme case $Re_\lambda = 1840$ we are able to resolve down to $\ell^* \simeq 10$ which is just at the border of the dissipative range [25]. In Figure 2, the second and fourth-order structure functions obtained for $Re_\lambda = 230$ and for $Re_\lambda = 1840$ compensated with the scaling behavior (1) are plotted (Kolmogorov length and velocity scales are used to adimensionalise the horizontal and vertical axes). The large scale asymptotic values are also functions of the Reynolds number and, for the second-order structure functions, increase almost linearly as Re_λ ; this result is in agreement with that simply derived by dimensional arguments on *rms* and Kolmogorov velocities, i.e. that $u'^2 / \langle \delta u(\eta)^2 \rangle \sim Re_\lambda$. Scaling exponents can be derived from structure functions of Figure 2 within the inertial range (approximately from $\ell \simeq 80$ to $\ell \simeq 500$, using a criterion based on 3% difference from the maximum in the third-order structure function divided by ℓ). The results ($\zeta_2 = 0.708 \pm 0.020$ and $\zeta_4 = 1.265 \pm 0.035$ for $Re_\lambda = 230$) agree with those obtained numerically and experimentally by other authors [4].

IV. RESULTS AND COMPARISON WITH THEORETICAL PREDICTIONS

In Figure 3 we plot the average surrogate energy dissipation $\langle E(\ell) \rangle$, computed from (10) and adimensionalized with large scale quantity u^3/L , as a function of Re_λ . A constant value of energy dissipation is expected from energy balance arguments [3]. Thus, the observed independence of $\langle E(\ell) \rangle$, computed at fixed $\ell^* = 10$, on Re_λ is a confirmation that the dissipative scales are resolved. We can give a different estimation of the dissipation on the basis of the energy spectrum. The advantage in this case is that we can reduce the noise by interpolation of the spectrum down to the dissipative scales [3,25]. The result for our data, also plotted in Figure 3, is consistent with the previous one thus confirming that the evaluation of the energy dissipation statistics from the present data is reliable.

In order to verify the prediction for θ_p of Section II, the scaling laws (12) of the moments of $E(\ell)$ with Re_λ must be computed. In Figure 4, an example of this scaling, computed at $\ell^* = 10$, is given for different values of p . We are confident that at least up to $p = 3$ the scaling exponents can be evaluated with an error on the fit less than 5%.

The resulting exponents θ_p are given in Figure 5. They have been computed at two different values of the separation $\ell^* = 10, 100$. As expected, for separations moving from the dissipative range into the inertial range, the curve of the exponents $\theta(p)$ becomes flatter and approaches the prediction (13). In Figure 5 we also plot the two predictions (9) and (13). These are been obtained by computing the structure function scaling exponents ζ_q (1) as discussed above, at the largest Re_λ available. Given the exponents ζ_q , the codimension $Z(h)$ has been obtained by numerical inversion of (4). Finally, (9) is used to predict the values of θ_p .

The agreement of our data with the two predictions (12) and (13) is remarkable. The value of θ_p obtained from $E(\ell)$ at $\ell^* = 10$ are very close to prediction (9-12). Some deviations are observed, starting from moment $p \simeq 2.5$. These are probably due to the relatively large value of $\ell^* = 10$, which is at the border of the dissipative range and to the statistics. Indeed, according to (10), the computation of θ_3 corresponds roughly to the computation of the 6-th

order structure function.

Let us remark again that the difference between predictions (9) and (13) is based on the assumption of a dissipative scale fluctuating with the local energy dissipation. Our experimental data demonstrate that this is indeed the case.

V. REMARKS AND CONCLUSIONS

In this paper, the scaling of velocity increments at very small scales in a turbulent flow is investigated with special focus on Reynolds number dependence. Within the multifractal framework it is possible to derive a relation between the scaling of the energy dissipation statistics with the Reynolds number and the scaling exponents of the velocity structure functions at fixed Reynolds number. This relation is found to fit very well experimental data taken into a water jet over about a decade of Re_λ . The one-dimensional surrogate of energy dissipation is estimated from velocity differences at very small scale, at the border of the dissipative range. It is shown that our statistics changes from prediction (12) to prediction (13) as the separation ℓ moves into the inertial range. The difference between the two predictions is the demonstration of the fluctuation of the dissipative scale.

A Reynolds number dependence of the moments of the velocity increments also in the limit of very high values ($Re_\lambda > 1000$) has been recently reported by different authors [6]. Due to the fact that the Reynolds number is expected to affect mainly the dissipative scales, the previous findings confirm experimentally the connection between small and inertial range scalings. This could support ESS (for example in respect to the enhanced range of scales involved), but simultaneously invalidate it (in respect of the independence on the Reynolds number). If these results are dependent on the still finite value of the Reynolds number or on the anisotropy of the flow field is left as a subject for future investigations.

REFERENCES

- [1] F. Anselmet, Y. Gagne, E.J. Hopfinger and R.A. Antonia, *J. Fluid Mech.*, **140**, 63 (1984).
- [2] A. Vincent and M. Meneguzzi, *J. Fluid Mech.*, **225**, 1 (1991).
- [3] A.S. Monin and A.M. Yaglom, *Statistical Fluid Mechanics*, MIT Press, Cambridge, MA (1975).
- [4] U. Frisch, *Turbulence*, Cambridge Univ. Press, Cambridge, UK (1995).
- [5] R.A. Antonia, T. Zhou and G. Xu, *Phys. Fluids*, **12**, 1509 (2000).
- [6] R.A. Antonia, B. Pearson and T. Zhou, *Phys. Fluids*, **12**, 3000 (2000).
- [7] A. Arneodo et al., *Europhys. Lett.*, **34**, 411 (1996).
- [8] K.R. Sreenivasan, *Phys. Fluids*, **27**, 1048 (1984).
- [9] K.R. Sreenivasan, *Phys. Fluids*, **10**, 528 (1998).
- [10] C. Meneveau and K.R. Sreenivasan, *Phys. Rev. Lett.*, **59**, 1424 (1987).
- [11] C. Meneveau and K.R. Sreenivasan, *J. Fluid Mech.*, **224**, 429 (1991).
- [12] R. Benzi, L. Biferale, G. Paladin, A. Vulpiani and M. Vergassola, *Phys. Rev. Lett.*, **67**, 2299 (1991).
- [13] K. Kailasnath, K.R. Sreenivasan and G. Stolovitzky, *Phys. Rev. Lett.*, **68**, 2766 (1992).
- [14] P. Tabeling, G. Zocchi, F. Belin, J. Maurer and H. Willaime, *Phys. Rev. E*, **53**, 1613 (1996).
- [15] G. Parisi and U. Frisch, in *Turbulence and Predictability in Geophysical Fluid Dynamics, Proceed. Intern. School of Physics 'E. Fermi', 1983*, eds. M. Ghil, R. Benzi and G. Parisi, North-Holland, Amsterdam.

- [16] G. Paladin and A. Vulpiani, *Phys. Rev. A*, **35**, 1971 (1987).
- [17] U. Frisch and M. Vergassola, *Europhys. Lett.*, **14**, 439 (1991).
- [18] M. Nelkin, *Phys. Rev. A*, **42**, 7226 (1990).
- [19] J. Eggers and S. Grossmann, *Phys. Rev. A*, **45**, 2360 (1992).
- [20]
- [21] G. Boffetta, A. Celani and D. Roagna, *Phys. Rev. E*, **61**, 3234 (2000).
- [22] G.P. Romano and R.A. Antonia, *J. Fluid Mech.*, **436**, 231 (2001).
- [23] R.A. Antonia, T. Zhou and G.P. Romano, *Phys. Fluids*, **9**, 3465 (1997).
- [24] R.A. Antonia and B. Pearson, *Phys. Rev. E*, **62**, 8086 (2000).
- [25] R.A. Antonia and B. Pearson, *Flow Turbulence and Combustion*, **64**, 95 (2000).

TABLES

Outlet mean velocity U_0 (cm/s)	102	196	304	487	1060
Re_d	20400	39200	60800	97400	212000
Local mean velocity U (cm/s)	15.3	30.4	41.4	72.1	167
Local <i>rms</i> velocity u' (cm/s)	4.4	9.2	12.3	23.8	50.1
Re_λ	230	308	435	926	1840
Local integral scale L (cm)	5.5	6.3	9.4	22.0	41.1
Local Kolmogorov scale η (cm)	0.0181	0.0097	0.0086	0.0066	0.0045

TABLE I. Parameters of the experiments on the jet at $x/d = 40$ (except for the outlet mean velocity and the exit Reynolds number computed at $x/d = 0$).

FIGURES

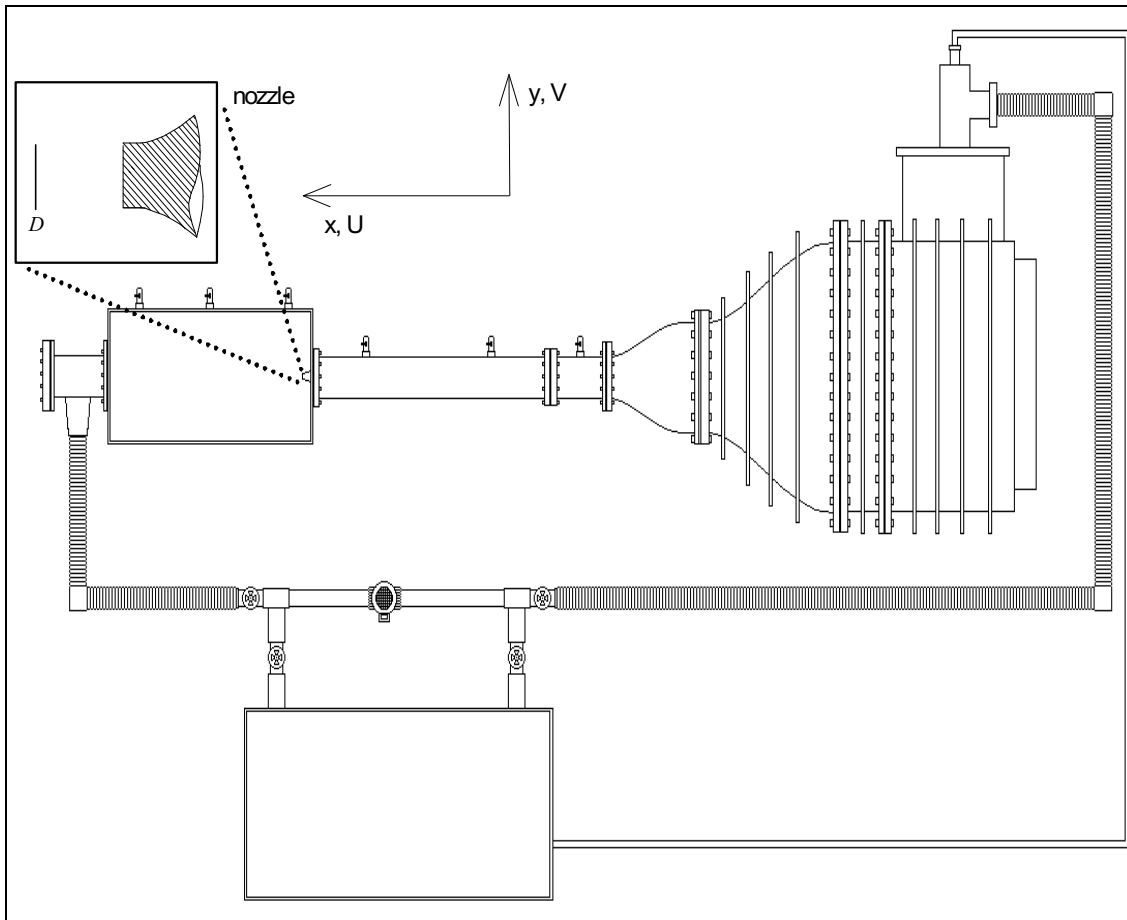


FIG. 1. Sketch of the experimental setup.

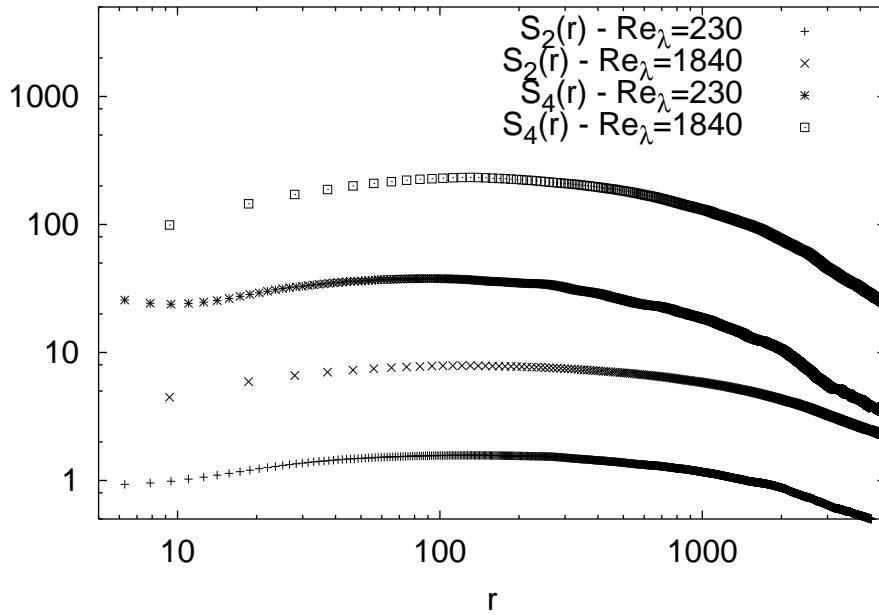


FIG. 2. Structure function of order 2 and 4 for different values of Re_λ compensated with the scaling behavior (1). The x-axis is adimensionalized with the Kolmogorov scale.

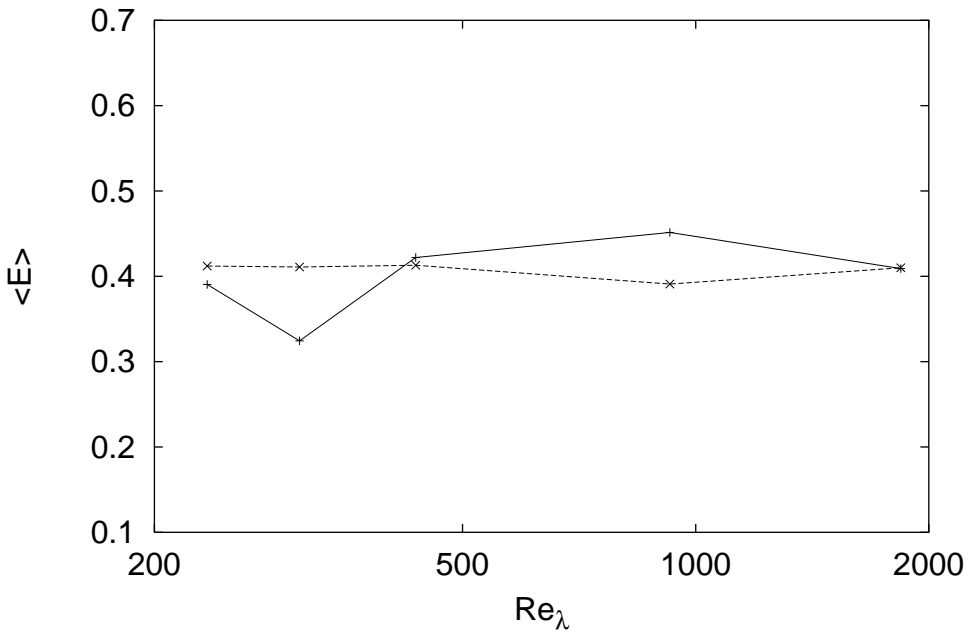


FIG. 3. Average energy dissipation computed from definition (10) (+) at $\ell^* = 10$ and from the energy spectrum (\times) as function of Re_λ .

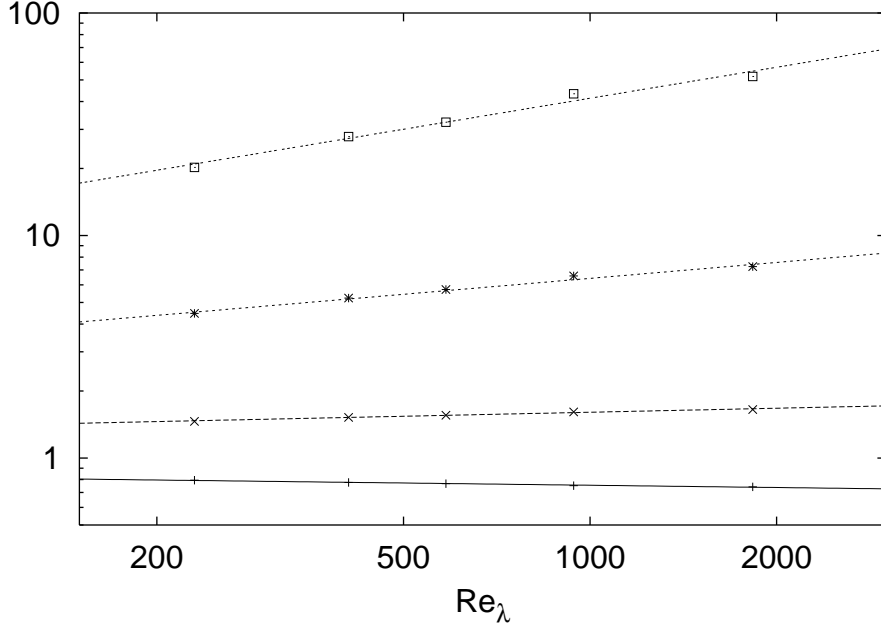


FIG. 4. Re_λ dependence of $\langle E(\ell)^p \rangle$ normalized with $\langle E(\ell) \rangle^p$ for $p = 2/3$ (+), $p = 4/3$ (\times), $p = 2$ (*) and $p = 8/3$ (\square) at $\ell = 10\eta$. The lines represent the best fit with a power law.

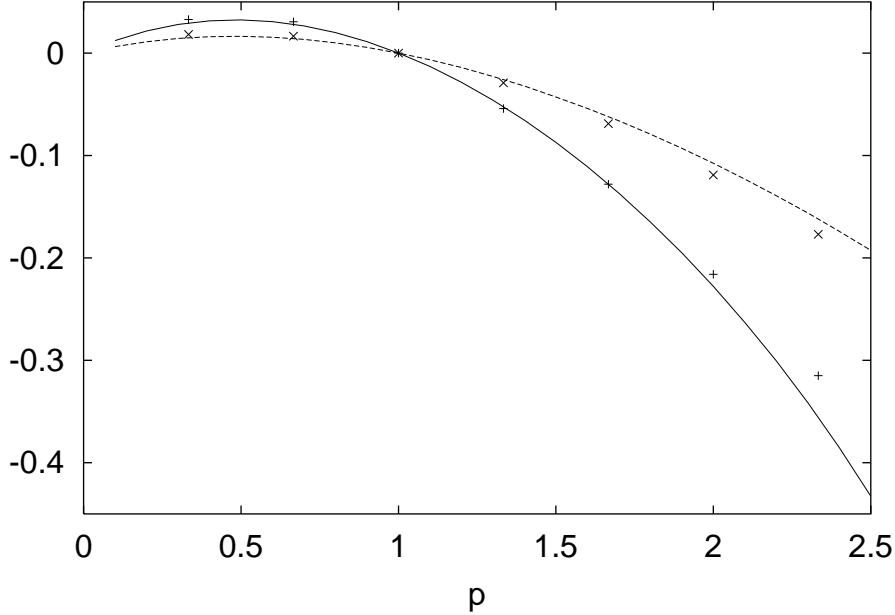


FIG. 5. Exponents θ_p obtained from the data of Figure 4 for $\ell = 10\eta$ (+) and $\ell = 100\eta$ (\times). The continuous line is the intermittent prediction (9), the dashed line is the prediction (13).